Studying the real-time interplay between triglyceride digestion and lipophilic micronutrient bioaccessibility using droplet microfluidics. 2 Application to various oils and (pro)vitamins

Thanh Hoang, Mélanie Nguyen, Marc Marquis, Sébastien Anton, Hoang Thanh Nguyen, Mélanie Marquis, Marc Anton, S. Marze

Studying the real-time interplay between triglyceride digestion and lipophilic micronutrient bioaccessibility using droplet microfluidics. 2 Application to various oils and (pro)vitamins

Hoang Thanh NGUYEN, Mélanie MARQUIS, Marc ANTON, Sébastien MARZE
Biopolymères Interactions Assemblages, INRA, 44300 Nantes, France

Abstract

The kinetics of micellar solubilization of lipophilic micronutrients (bioaccessibility) in relation with triglyceride digestion remains poorly known. To study this interplay in real-time, a droplet microfluidic method was designed and used as reported in the first part of this article series. In this second part, the interplay between the micellar solubilization of (pro)vitamins (beta-carotene or retinyl palmitate) and the digestion of triglyceride oils (tricaprylin TC, or high-oleic sunflower seed oil HOSO, or fish oil FO) during simulated gastrointestinal digestion was investigated. The relation between the release of both micronutrients and of triglyceride lipolytic products was found to be non-linear. The kinetics of beta-carotene was found to follow the kinetics of lipolytic products, depending on the oil type (TC > HOSO > FO). The effect of the gastric phase on the intestinal phase was also found to follow this order, mostly due to partial lipolysis during the gastric phase.

1. Introduction

Micronutrients (minerals, vitamins) are essential to maintain normal functions of human body. However, their absorption, especially that of lipophilic vitamins and carotenoids, is much more variable than that of macronutrients, due to biological and physicochemical factors (Borel, 2003). In the fat-soluble micronutrient class, vitamin A has received an intensive research attention due to its multiple functions in normal growth and development of human body. Vitamin A is notably involved in immune system maintenance, vision health and regulation of cell division (Grune et al., 2010; Haskell, 2012). Vitamin A is present in food in two forms: pre-formed vitamin A (mostly as retinyl palmitate) from animal sources, and provitamin A carotenoids (carotenes, beta-cryptoxanthin) from plant sources. Among provitamin A carotenoids, beta-carotene has the highest vitamin A activity thanks to its unique symmetrical structure (Grune et al., 2010; Haskell, 2012). Nevertheless, in order to achieve their vitamin activity, they need to be available in tissues (bioavailability), what requires many processes: i) release from the food matrix and incorporation in triglyceride droplets, ii) co-digestion with triglycerides, then co-solubilization into mixed micelles (bioaccessibility), iii) transport, processing, and secretion by intestinal cells iv) circulation in

the lymph or blood system in lipoprotein. Among these processes, the micellar solubilization is an important prerequisite for transport. However, because fat-soluble micronutrients are poorly soluble in the aqueous gastrointestinal environment, their bioaccessibility may be low and variable depending on many factors involving the food matrix structure and composition (Borel, 2003). Improving bioaccessibility is thus a strategy to enhance the bioavailability of these lipophilic micronutrients.

For the last couple of decades, many works based on *in vitro* digestion were carried out to study the bioaccessibility of beta-carotene in relation with triglyceride digestion (Huo, Ferruzzi, Schwartz, & Failla, 2007; Yi, Zhong, Zhang, Yokoyama, & Zhao, 2015). However, the interplay between the micellar solubilization of lipophilic micronutrients and of lipolytic products remains poorly known. For that matter, emulsion kinetic studies provided insights into the mechanisms of micellar solubilization of beta-carotene (Borel et al., 1996; Nik, Corredig, & Wright, 2011; Mutsokoti et al., 2017; Verkempinck et al., 2017). Better than a single end-point measurement, the release profile of bioactive molecules can be obtained by analyzing different incubation time points, but this is challenging due to difficulties in the control of experimental parameters using emulsion, the amount of materials needed, and the required high number of time points. Alternative approaches are scarce and the simultaneous real-time kinetics were established only once, using multiplex coherent Anti-Stokes Raman scattering microspectroscopy (Day, Rago, Domke, Velikov, & Bonn, 2010).

These issues can also be solved using droplet microfluidics. In the first part of this article series, we proposed a lab on a chip method enabling the simultaneous monitoring of beta-carotene and of tricaprylin lipolytic products in real time. In this second part, we extend this microfluidic approach to other oils and lipophilic micronutrients in order to understand their roles on the kinetic solubilization interplay. Three oils and two (pro)vitamins were tested separately, among which 5 systems were investigated. The full relation between the micellar solubilization of oil lipolytic products and of these micronutrients was established. The effect of the gastric phase on the subsequent intestinal phase was investigated as well.

2. Experimental Section

2.a. Materials

Pancreatic lipase (L3126, lipase from porcine pancreas type II, 1.7-8.3 U mg^{-1}), Amano lipase A (534781, lipase from Aspergillus niger, 12 U mg^{-1}, protease activity $\leq$ 2.5 U mg^{-1}), pepsin (P7012, pepsin from porcine gastric mucosa, 2500 U mg^{-1}), sodium glycodeoxycholate (G9910), tricaprylin TC (T9126), beta-carotene (22040), retinyl palmitate

RP (R1512) were provided by Sigma-Aldrich. High-oleic sunflower seed oil HOSO was provided by Vandamme (Belgium). Fish oil FO (1050 TG) was provided by Polaris (France).

2.b. Droplet digestion and lipid monitoring

In this work, digestion of oil droplets containing an added micronutrient was performed using the same microfluidic method described in detail in the first part of this article series. Briefly, monodisperse oil droplets of 100 µm containing an added micronutrient were generated/immobilized in a lab on chip device and then subjected to a semi-dynamic gastrointestinal digestion in the same chip, with a continuous flow (and thus renewal) of the digestive fluids at a flow rate of 50 µL min^{-1}. The digestion of the trapped oil droplets was carried out under controlled temperature of 37 °C inside the digestion chamber, and monitored in real-time (2 min time steps) using a confocal fluorescence microscope (Nikon A1+) with a 10× objective. All optical parameters were optimized to obtain auto fluorescence intensity of the different micronutrients for quantitative analysis. A laser with an excitation wavelength of 488 nm and a channel with emission window of 500-530 nm were used to obtain the autofluorescence image of BC inside the oil droplets. A transmitted light image for the droplet size was obtained simultaneously using the same excitation beam. Due to its different absorption and emission properties compared to those of BC, a laser with an excitation wavelength of 375 nm and a channel with an emission window of 425-475 nm were used to obtain the autofluorescence image of RP. A transmitted light image for the droplet size was obtained simultaneously using the 488 nm laser already used for BC. The droplet size and fluorescence were measured by image analysis. Micronutrient concentration and release were calculated from these values using a fluorescence calibration curve as explained in the first part of this series.

The digestion was run with either an intestinal phase alone or a gastric phase followed by an intestinal phase. The intestinal fluid was prepared by mixing a buffer solution (100 mM NaH_2PO_4 adjusted to pH 7.0) with pancreatic lipase at 4 mg mL^{-1} and a bile salt (sodium glycodeoxycholate) at 5 mg mL^{-1}. When a gastric phase was performed prior to the intestinal phase, it was carried out for 2 hours with a gastric fluid prepared by mixing 0.03 mg mL^{-1} lipase from *Aspergillus niger* (lipase AN), and 0.6 mg mL^{-1} pepsin in a 100 mM KCl buffer adjusted to pH 3.0.

Three triglycerides composed of different fatty acids were tested: pure tricaprylin (TC, C8:0), or high-oleic sunflower seed oil (HOSO, mainly C18:1), or a fish oil rich in DHA (FO, mainly C22:6). Two micronutrients were tested separately (same initial concentration of 0.2 wt% in the oils): beta-carotene (provitamin A) or retinyl palmitate (preformed vitamin A). For each system, two to three independent digestions were conducted with the monitoring of seven individual droplets for each digestion. A distinct microfluidic device was used for each

digestion to ensure identical initial conditions. The variability of the measurements was very low between the seven droplets monitored during one digestion, so the error bar (plotted as the standard deviation) represents the variability of the two to three independent digestions.

3. Results and discussion

3.a. Intestinal phase

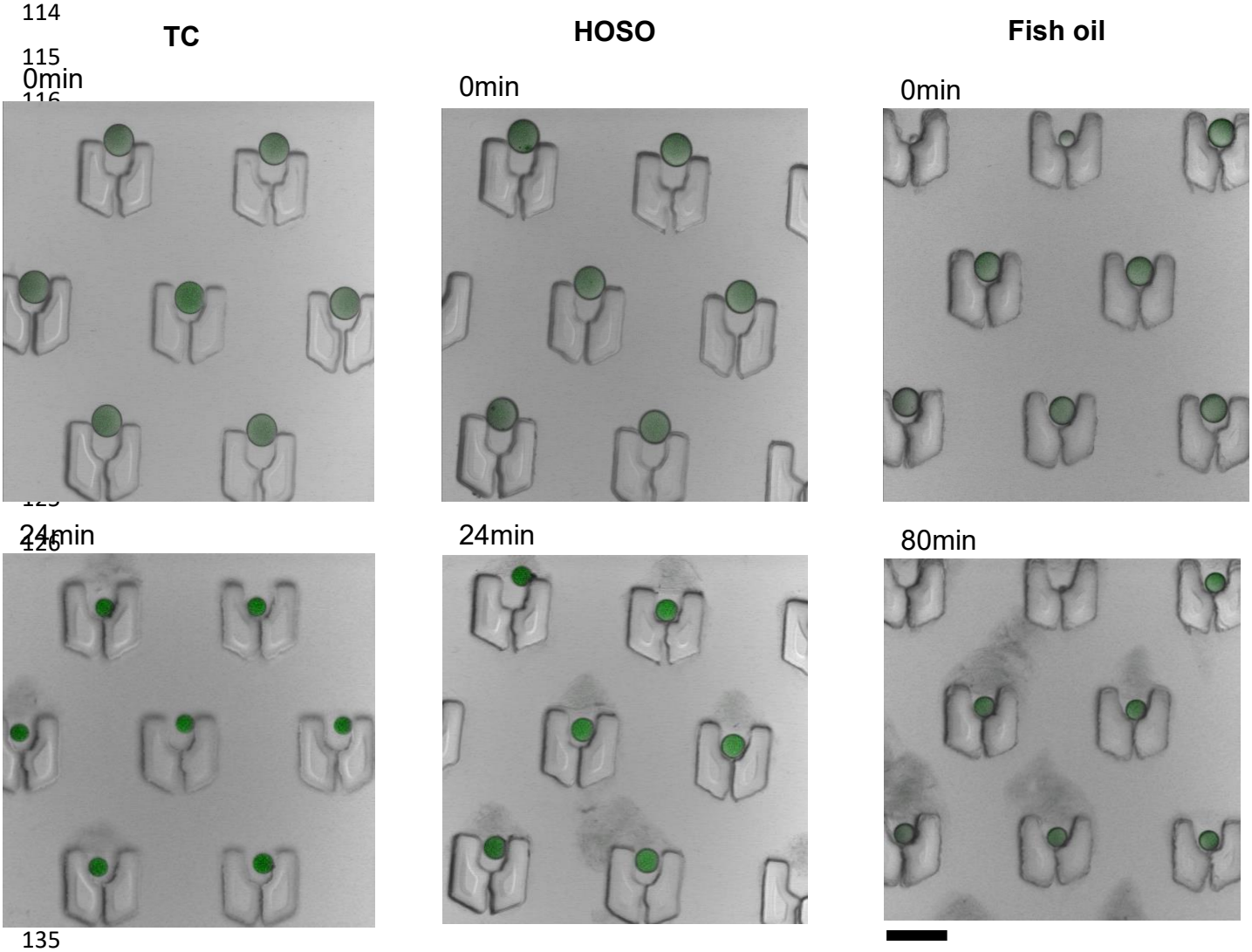

Fig. 1 Images of droplets containing beta-carotene for different oils (TC, HOSO, fish oil) at various intestinal digestion times. The scale bar represents 200 µm.

Digestion of TC, HOSO, and fish oil containing the same initial BC concentration (0.2 wt%) were conducted. Fig. 1 shows the evolution of droplet size and fluorescence for different oils

during the intestinal digestion. The reduction of the droplet size comes from the lipolysis of triglycerides into free fatty acids and monoglycerides, which exit the droplet as they can solubilize in the aqueous bile salt micelles.

The digestion kinetics of the three oils is shown in fig. 2a. The fastest rate is found for TC and the slowest rate for fish oil. This is due to higher lipase activity and bile salt solubilization capacity for short saturated fatty acid chains (TC) compared to long polyunsaturated fatty acid chains (fish oil), as already reviewed (Marze, 2014). Calculations were done to quantify the free fatty acid (FFA) release rate during the intestinal digestion. The mathematical model is detailed in the supplementary material S1. Assuming the FFA release rate is proportional to the surface area of the oil droplet (Li & Mcclements, 2010; Marze & Choimet, 2012; Gaucel, Trelea, & Le Feunteun, 2015), the equation we used reads:

$$R(t) = R_0\left(1 - \frac{k_S M_W}{2R_0\rho}t\right) \qquad (1)$$

where k_s is the FFA release rate per unit droplet surface area (mol s^{-1} m^{-2}), ρ is the density of the triglyceride oil droplet (g m^{-3}), M_W is the molecular weight of the triglyceride oil (g mol^{-1}), t is the time (s), and R_0 is the initial radius of the oil droplet (m).

Note that a similar equation accounting for the total reaction volume is derived in the supplementary material S1. These models were systematically applied to pH-stat measurements of emulsion lipolysis. The comprehensive fitted release rates for microfluidic droplets and for emulsions are compared in the supplementary material S2.

The FFA release rate per droplet surface area was determined using eq. (1). The rates were of 41.2 ± 1.4, 13.2 ± 0.2, and 3.08 ± 0.01 µmol s^{-1} m^{-2} for TC, HOSO, and fish oil, respectively. These values are about 35% lower than those obtained previously using droplet microfluidics (Marze, Algaba, & Marquis, 2014), but when the rates are normalized to HOSO, the ratios are of 3.1 and 0.23 for TC and fish oil, respectively, which are close to the ratios of 2.5 and 0.21 normalized to olive oil (Marze et al., 2014). The absolute rate values are about one-two orders of magnitude higher than those for emulsions (Li, & McClements, 2010, Marze, & Choimet, 2012, supplementary material S2). This difference is likely due to the absence of coalescence in our droplet microfluidic approach, whereas coalescence reduces the surface area available for lipolysis and solubilization in the case of emulsions, what is not accounted for in the models (supposing no coalescence).

The digestion rate also depends on both the lipase specificity for the triglycerides and the capacity of the bile salt to remove the lipolytic products from the droplet surface (solubilization of lipolytic products). In general, the longer the fatty acid chain, the lower the lipase activity and the lower the solubilization capacity for the lipolytic products (Marze, 2014). Lipase activity is actually dependent on solubilization capacity, as lipolytic products

accumulating at the droplet surface are known to inhibit further lipolysis (Pafumi et al., 2002). Hence, a lower solubilization capacity will induce a lower apparent lipolysis rate. In these microfluidic experiments, the continuous renewal of the intestinal fluid results in a large excess of bile salts, thus lipolysis is likely the limiting step. This is confirmed by comparing the results of this single droplet study to emulsion lipolysis experiments with optimized bile salt concentrations (Marze, 2014). The relative rates normalized to HOSO (3.1 and 0.23 for TC and fish oil, respectively) are indeed in the same range.

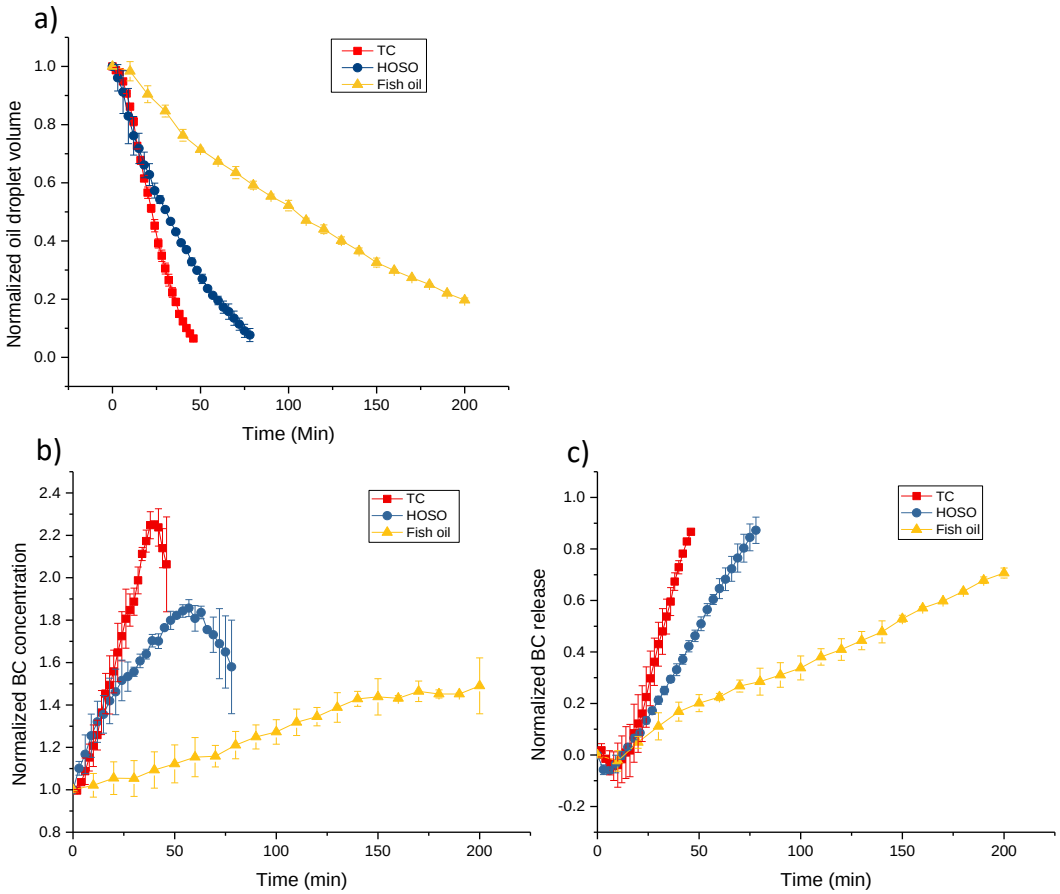

Fig. 2 a) Evolution of the normalized droplet volume, b) evolution of the normalized BC concentration inside the droplets, and c) evolution of BC proportion released from the droplets for different oils (TC, HOSO, Fish oil) during intestinal digestion.

In fig. 2b, the concentration of BC in the droplets during intestinal digestion for the three oils is reported. For TC and HOSO, BC concentration mainly increases during digestion, reaching a maximum and then decreases near the end of the digestion. For fish oil, the decreasing part was not observed due to a much longer digestion time. Such increasing trend for vitamin D3 concentration inside TC droplets was reported for emulsions, but no

196 decrease was observed because the digestions were incomplete (Day et al., 2010). The
197 increase of BC inside the oil droplets could be explained by the competition between BC and
198 lipolytic products for solubilization into the bile salt micelles, knowing that their solubilization
199 capacity is much lower for beta-carotene and retinol (about 5.10^{-4} and 6.10^{-3} mol/mol,
200 respectively) (El-Gorab, & Underwood, 1973), compared to fatty acids and monoglycerides
201 (range 4.10^{-2} – 3.5) (Marze, 2014). Differences in the kinetics of BC concentration for the
202 three oils are observed, as BC concentrates more in the droplets in the case of oils
203 undergoing faster lipolysis.
204 The evolution of BC release as a function of intestinal digestion time is presented in fig. 2c.
205 These results show that although BC concentration increases in the droplets, it is
206 nevertheless significantly released in all cases. Thus the concentration increase is due to a
207 slower BC release rate compared to the lipolytic products release rate. The maximal rates of
208 BC release from the oil droplet per unit droplet surface area were calculated from the BC
209 release and the droplet size data, of 0.57 ± 0.04, 0.25 ± 0.03, and 0.035 ± 0.008 µmol s^{-1} m^{-2}
210 for TC, HOSO, and fish oil, respectively. The BC release rates were found to follow the same
211 order as the lipolytic products release rates (TC > HOSO > FO). This is in agreement with
212 many studies showing higher bioaccessibility of various lipophilic compounds from medium-
213 chain triglycerides compared to long-chain triglycerides (Marze, 2015). For all three oils,
214 much higher final BC bioaccessibility values (about 90% in the cases of the fully digested TC
215 and HOSO) were found compared to values obtained for the static digestion of emulsions in
216 the literature (Nik et al., 2011; Mutsokoti et al., 2017; Verkempinck et al., 2017). This is likely
217 explained by the continuous renewal of the intestinal digestive fluid (semi-dynamic method),
218 providing bile salt micelles that are not saturated with lipolytic products and BC constantly, in
219 contrast with the static methods in which saturated bile salt micelles are not replaced. Note
220 that a porcine bile extract containing various bile salts was also tested instead of the single
221 bile salt, at the same total bile salt concentration. The kinetics were found to be significantly
222 faster only in the case of TC, probably because all bile salts formed mixed micelles efficiently
223 with medium-chain fatty acids and monoglycerides, as compared to long-chain ones (Marze,
224 2014).
225 As in the first article of this series, the relation between the micellar solubilization of BC and
226 of the lipolytic products is shown in fig. 3. First, we observe that this relation is almost linear
227 in the case of fish oil, but can be highly non-linear in the cases of TC and HOSO. The added
228 black dash line represents the “balance” case in which the BC release equals the lipolytic
229 products release (also named lipid release). All three curves lie below this black dash line, so
230 the relative mass release of BC is always lower compared to that of lipids, hence the
231 increase of the BC concentration inside the oil droplets observed in fig. 2b. Although the BC
232 release rate ranks like the lipid release rate, that is TC > HOSO > FO, the reverse is true

when BC mass release is compared to the lipid mass release. The curve of fig. 3 can be seen as a micronutrient release efficiency curve, where the closer the curve from the black dash line, the more efficient the triglyceride digestion is for BC release.

For retinyl palmitate, RP concentration trends inside the oil droplets and RP release were very similar to those for BC shown in figs. 2. The final RP release efficiency curves for two oils are compared to the case of BC in figs. 3b and 3c. The results show similar non-linear relations. A higher RP release efficiency compared to BC is observed in the first part of the digestion. However, this is only statistically significant in the case of HOSO due to much larger error bars for RP. These variations were explained by much larger fluctuations in the intensity of the 375 nm laser as compared to the 488 nm laser.

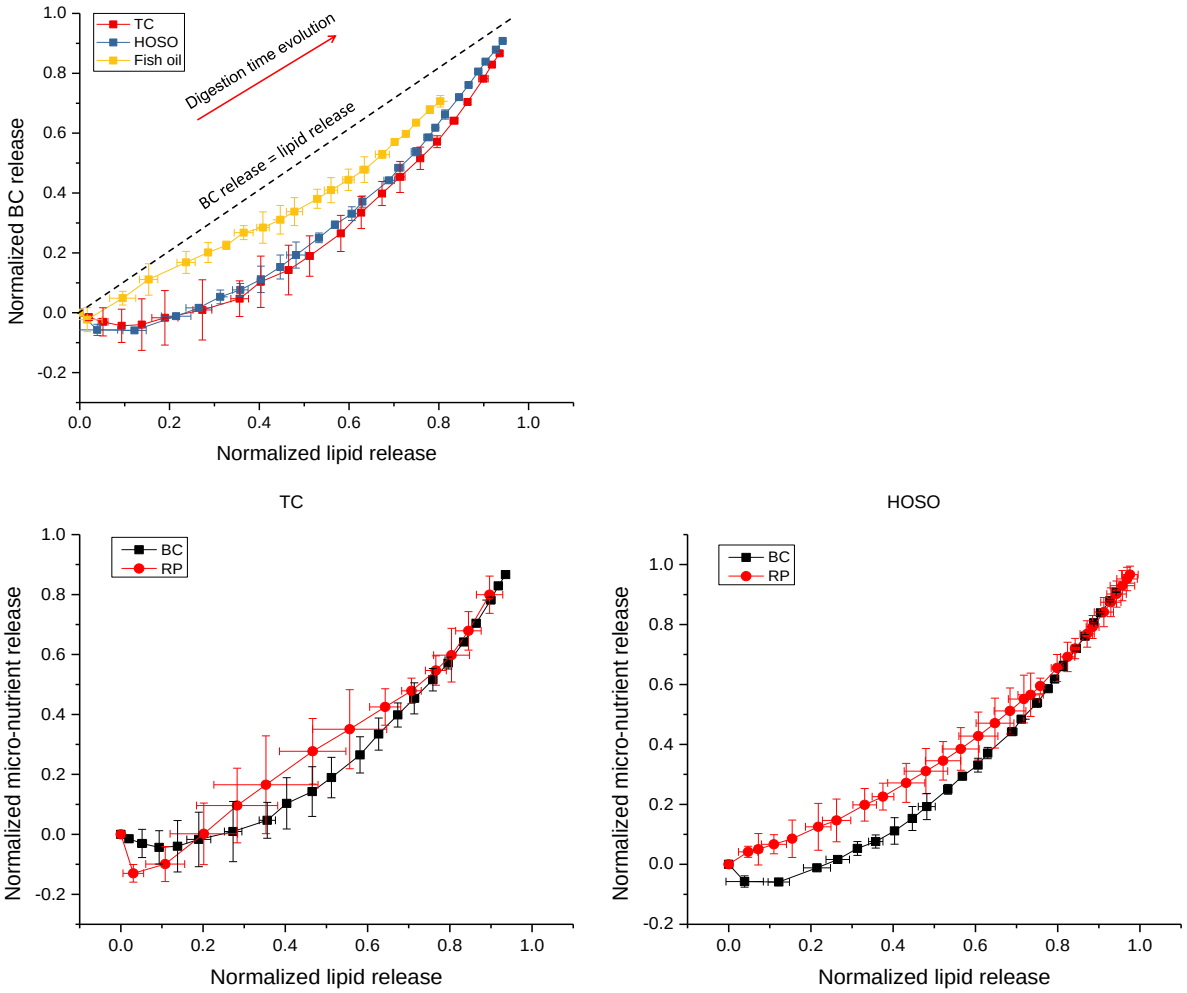

Fig. 3 a) Relation between the normalized mass release of BC and of lipids for different oils (TC, HOSO, fish oil), b) comparison between BC and RP release for TC, and c) comparison between BC and RP release for HOSO.

In the case of a fast initial lipolysis (TC and HOSO), the micronutrients must compete with more lipolytic products for solubilization in bile salt micelles. Thus, it leads to a low initial BC mass release. The curve for the fish oil is significantly different, showing that a slower initial lipolysis can induce a high initial BC mass release. In this case, there is more interplay between micronutrient release and lipid digestion, suggesting that cooperation prevails over competition. This is in agreement with the enhancement of the solubilization capacity of bile salt micelles by the formation of mixed micelles containing fatty acids and monoglycerides. This enhancement is indeed known to be much more efficient in the case of long polyunsaturated lipids compared to short saturated ones (Kossena, 2004). This could be understood on the basis of the formation of highly swollen mixed micelles accommodating large lipophilic molecules, or poorly swollen mixed micelles with lower solubilization capacity, respectively (Colle, 2012).

Similar to the case for TC discussed in the first article of the series, the BC release efficiency curve for HOSO was found to be non-linear with three different kinetic regimes. In contrast, strictly linear relations are often reported in emulsion digestion studies (Borel et al., 1996; Nik et al., 2011; Mutsokoti et al., 2017). This is likely due to the limited number of time points monitored using the emulsion approach. Indeed, most portions of the full efficiency curve will appear linear with scarce data points. In the contrary, very similar non-linear curves were obtained from agent-based simulations (Marze, 2014). In addition to the competition/cooperation interpretation, these simulations revealed that highly lipophilic molecules slowly diffuse inside the droplet. When the triglyceride digestion rate is slow, they statistically have enough time to reach the interface at the beginning of the digestion (ideal balance case and fish oil). When the triglyceride digestion rate is fast, they statistically reach the interface towards the end of the digestion, when the droplet size is small, hence the higher release in this regime.

3.b. Effect of the gastric phase

A gastric phase was added prior to the intestinal phase in order to investigate its effect. Fig. 4 shows the evolution of the normalized droplet volume as a function of digestion time during the gastric phase followed by the intestinal phase for the three oils. During the gastric phase, a decrease in the droplet volume was only observed for TC. Using eq. (1), the release rate of FFA per unit droplet surface area was calculated to be 9.7 ± 2.8 µmol s^{-1} m^{-2}, which is much lower than that during the intestinal phase (41.2 ± 1.4 µmol s^{-1} m^{-2}). These results are consistent with those reported by Marze et al., 2014 and can be explained by the much lower concentration of lipase AN compared to pancreatic lipase, and by the absence of bile salts in

the gastric phase. The lipolytic products of TC have a sufficiently high aqueous solubility to be removed from the interface in the absence of bile salt micelles, allowing interfacial lipase activity. In the contrary, the poorly water soluble lipolytic products of long-chain triglycerides (HOSO and fish oil) can actually not be solubilized in the aqueous phase and hence saturate the interface, allowing only partial lipolysis by inhibiting further lipase activity (Pafumi et al., 2002).

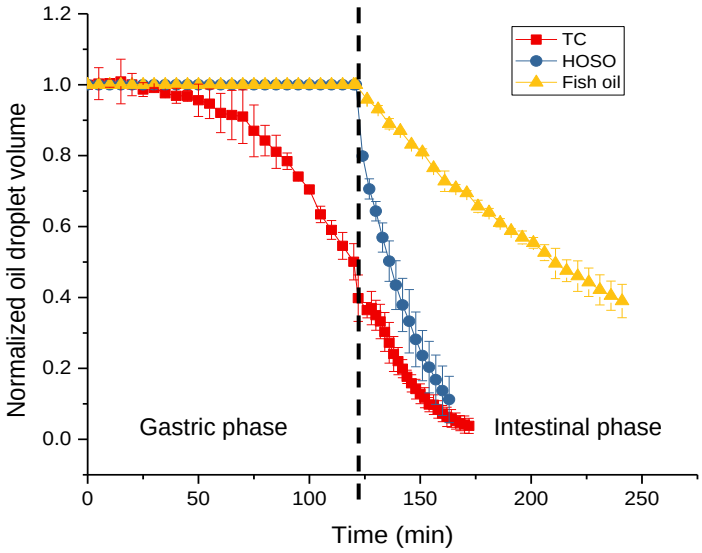

Fig. 4 Evolution of the normalized droplet volume for different oils (TC, HOSO, fish oil) as a function of digestion time, with a gastric phase before the intestinal phase.

In figs. 5, the evolution of the droplet volume during the intestinal phase (with or without a preceding gastric phase) is presented. It shows that the effect of the gastric phase depends on the oil. The shorter the chain length of the triglycerides is, the greater the effect. In the case of TC, the gastrointestinal digestion extent was always higher than the intestinal digestion alone, mainly due to the solubilization during the gastric phase. Indeed, when the droplet volume is renormalized at the start of the intestinal phase, the kinetics is only significantly faster at the beginning of the intestinal phase, with an initial steep decrease in the droplet volume. In the case of HOSO, an even steeper decrease is observed at the beginning of the intestinal phase following the gastric phase. This confirms that partial lipolysis occurred and lipolytic products accumulated at the droplet interface during the gastric phase, immediately removed by the bile salt micelles at the start of the intestinal phase, causing the steep decrease in the droplet volume. In the contrary, the gastric phase has almost no effect in the case of the fish oil. Those results are different from the ones

reported by Marze et al., 2014, in which the gastric phase had no effect on the following intestinal phase. This contradiction can be explained by different experimental parameters regarding the initial droplet size, the gastric fluid composition, and the gastric phase duration. In the current experiments, the initial droplet size was smaller (higher surface to volume ratio), pepsin was present in the gastric fluid, hydrolyzing the initial layer of beta-lactoglobulin, and the gastric phase duration was longer.

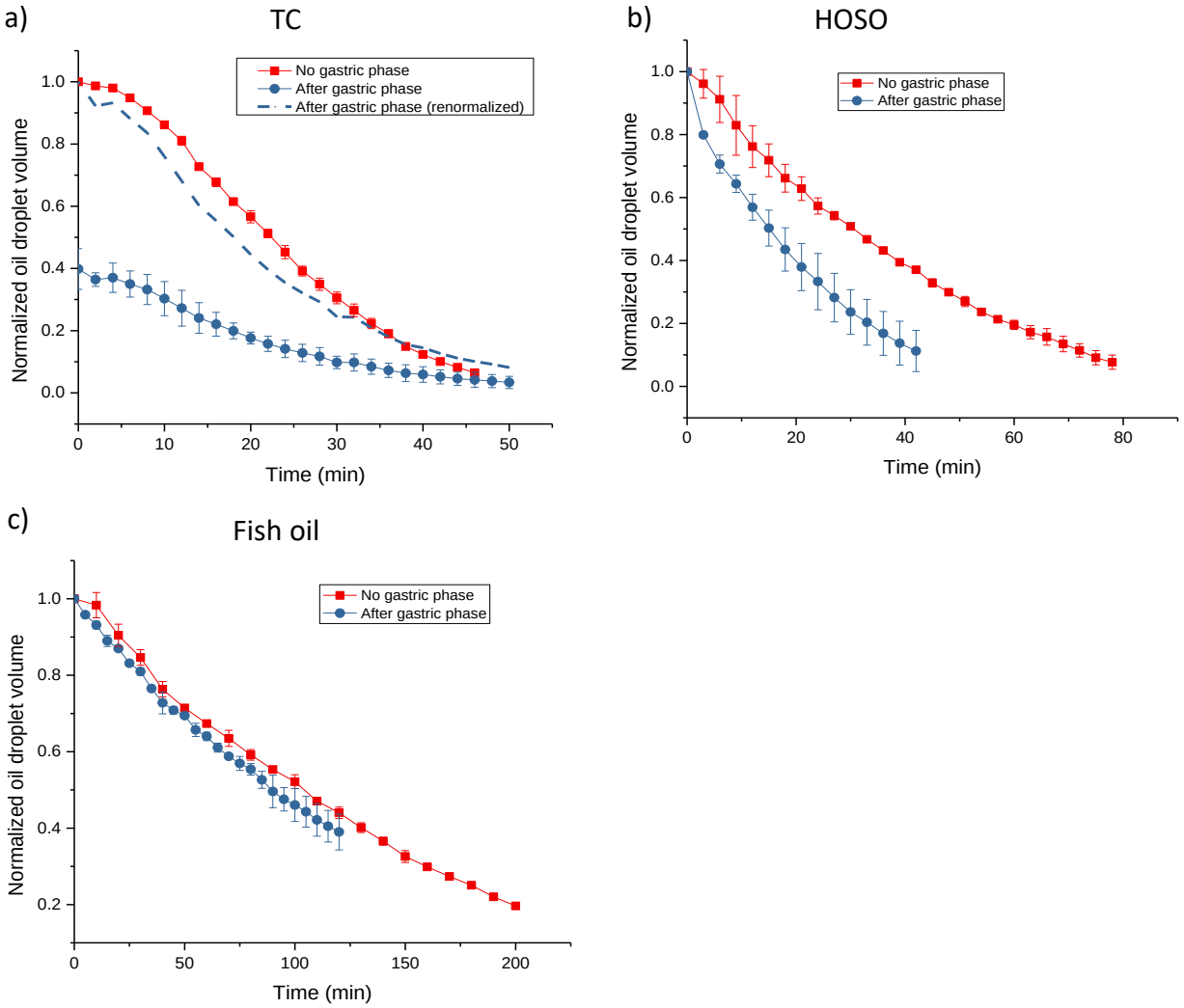

Fig. 5 Effect of the gastric phase on the intestinal phase of digestion for different oils: a) TC, b) HOSO, c) fish oil.

Figs. 6 show the effect of the gastric phase on the BC release from the oil droplets during the intestinal phase. For TC and HOSO, the BC release is significantly faster at the beginning of the intestinal phase when a preceding gastric phase was performed. For TC, this is likely due to the smaller size of the droplets, as discussed above. For HOSO, BC molecules could

localize in clusters of lipolytic products at the droplet surface, as postulated by Pafumi et al., 2002 for long-chain lipids. When the intestinal phase starts, the bile salt micelles would quickly solubilize these clusters, resulting in a fast release of both lipids and BC. For fish oil, no effect of the gastric phase on the BC release during the intestinal phase was observed.

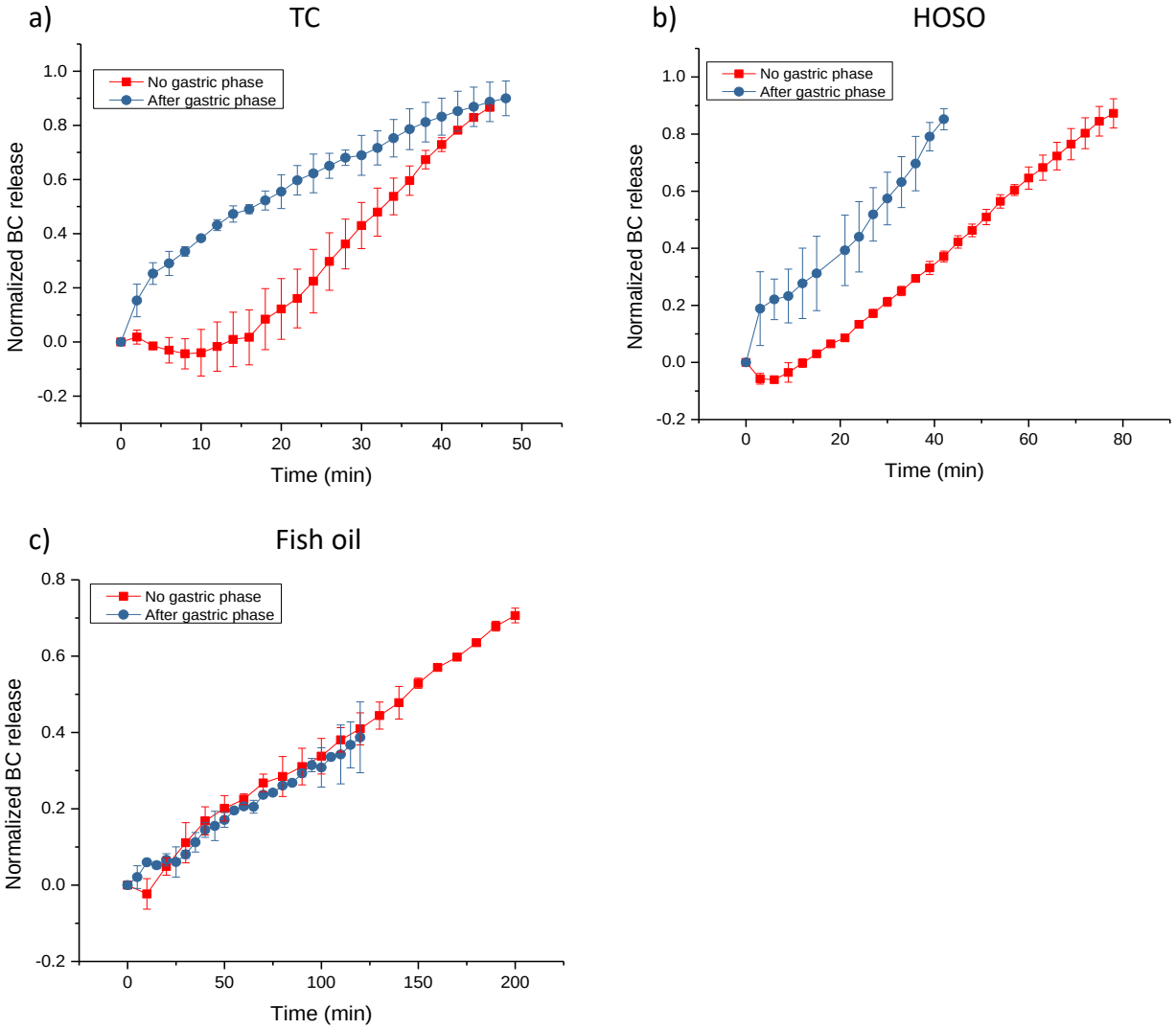

Fig. 6 Effect of the gastric phase on BC release from the droplets during the intestinal phase of digestion for different oils: a) TC, b) HOSO, c) fish oil.

Conclusion

The full kinetic relation between the release of micronutrients and the release of lipolytic products was found to be non-linear for both BC and RP. The bioaccessibility kinetics of both micronutrients depended on the type of fatty acid. BC added to the quickly digested oil (TC, with a short saturated fatty acid chain) presented a lower release efficiency compared to BC

added in the slowly digested oil (fish oil, with long polyunsaturated fatty acid chains). The interplay between the bioaccessibility of micronutrients and the lipolysis of triglycerides was interpreted on the basis of micellar solubilization competition/cooperation and of digestion/diffusion time comparisons. The effect of the gastric phase before the intestinal phase was also found to depend on the fatty acid type.

These results could be used to design delivery systems with controlled release properties based on the oil-micronutrient association. Overall, these results show the need for real-time kinetics studies of lipophilic micronutrients to provide insights about their fate in the gastrointestinal tract. This knowledge will enable a better understanding and improvement of the bioaccessibility of lipophilic micronutrients, and in turn could prove essential to control their bioavailability.

References

Borel, P. (2003). Factors affecting intestinal absorption of highly lipophilic food microconstituents (fat-soluble vitamins, carotenoids and phytosterols). *Clinical Chemistry and Laboratory Medicine*, *41*(8), 979–994.

Borel, P., Grolier, P., Armand, M., Partier, A., Lafont, H., Lairon, D., & Azais-Braesco, V. (1996). Carotenoids in biological emulsions: Solubility, surface-to-core distribution, and release from lipid droplets. *Journal of Lipid Research*, *37*(2), 250–261.

Colle, I. J. P., Van Buggenhout, S., Lemmens, L., Van Loey, A. M., & Hendrickx, M. E. (2012). The type and quantity of lipids present during digestion influence the in vitro bioaccessibility of lycopene from raw tomato pulp. *Food Research International*, *45*(1), 250–255.

Day, J. P. R., Rago, G., Domke, K. F., Velikov, K. P., & Bonn, M. (2010). Label-free imaging of lipophilic bioactive molecules during lipid digestion by multiplex coherent anti-stokes raman scattering microspectroscopy. *Journal of the American Chemical Society*, *132*(24), 8433–8439.

El-Gorab, M., & Underwood, B. A. (1973). Solubilization of beta-carotene and retinol into aqueous solutions of mixed micelles, *306*, 58–66.

Giang, T. M., Gaucel, S., Brestaz, P., Anton, M., Meynier, A., Trelea, I. C., & Le Feunteun, S. (2016). Dynamic modeling of in vitro lipid digestion: individual fatty acid release and bioaccessibility kinetics. *Food Chemistry*, *194*, 1180–1188.

Grune, T., Lietz, G., Palou, A., Ross, A. C., Stahl, W., Tang, G., … Biesalski, H. K. (2010). Beta-carotene is an important vitamin A source for humans. *The Journal of Nutrition*, *140*(12), 2268S–2285S.

Haskell, M. J. (2012). The challenge to reach nutritional adequacy for vitamin A: β-carotene bioavailability and conversion - Evidence in humans. *American Journal of Clinical*

Nutrition, *96*(5), 1193S-1203S.

Huo, T., Ferruzzi, M. G., Schwartz, S. J., & Failla, M. L. (2007). Impact of fatty acyl composition and quantity of triglycerides on bioaccessibility of dietary carotenoids. *Journal of Agricultural and Food Chemistry*, *55*(22), 8950–8957.

Kossena, G. A., Charman, W. N., Boyd, B. J., Dunstan, D. E., & Porter, C. J. H. (2004). Probing Drug Solubilization Patterns in the Gastrointestinal Tract after Administration of Lipid-Based Delivery Systems: A Phase Diagram Approach. *Journal of Pharmaceutical Sciences*, *93*(2), 332–348.

Li, Y., & Mcclements, D. J. (2010). New mathematical model for interpreting ph-stat digestion profiles: Impact of lipid droplet characteristics on in vitro digestibility. *Journal of Agricultural and Food Chemistry*, *58*(13), 8085–8092.

Marze, S., & Choimet, M. (2012). In vitro digestion of emulsions: Mechanistic and experimental models. *Soft Matter*, *8*(42), 10982–10993.

Marze, S. (2014). A coarse-grained simulation to study the digestion and bioaccessibility of lipophilic nutrients and micronutrients in emulsion. *Food Funct.*, *5*(1), 129–139.

Marze, S., Algaba, H., & Marquis, M. (2014). A microfluidic device to study the digestion of trapped lipid droplets. *Food Funct.*, *5*(7), 1481–1488.

Mutsokoti, L., Panozzo, A., Pallares Pallares, A., Jaiswal, S., Van Loey, A., Grauwet, T., & Hendrickx, M. (2017). Carotenoid bioaccessibility and the relation to lipid digestion: A kinetic study. *Food Chemistry*, *232*, 124–134.

Nik, A. M., Corredig, M., & Wright, A. J. (2011). Release of lipophilic molecules during in vitro digestion of soy protein-stabilized emulsions. *Molecular Nutrition and Food Research*, *55*(SUPPL. 2), 278–289.

Pafumi, Y., Lairon, D., De La Porte, P. L., Juhel, C., Storch, J., Hamosh, M., & Armand, M. (2002). Mechanisms of inhibition of triacylglycerol hydrolysis by human gastric lipase. *Journal of Biological Chemistry*, *277*(31), 28070–28079.

Yi, J., Zhong, F., Zhang, Y., Yokoyama, W., & Zhao, L. (2015). Effects of Lipids on in Vitro Release and Cellular Uptake of β-Carotene in Nanoemulsion-Based Delivery Systems. *Journal of Agricultural and Food Chemistry*, *63*(50), 10831–10837.

Mathematical models for the FFA release

Calculations were done to quantify the free fatty acid (FFA) release rate during the intestinal digestion. Assuming the FFA release rate is proportional to the surface area of the oil droplet (Li & Mcclements, 2010; Marze & Choimet, 2012; Gaucel et al., 2015), the number of moles of FFA released from the droplet per unit time (mol s^{-1}) is written:

$$\frac{dN_{FFA}}{dt} = k_S S \quad (1)$$

where S is the droplet surface area (m^2), and k_s is the FFA release rate per unit droplet surface area (mol s^{-1} m^{-2}).

As the lipolysis of one triglyceride (TG) molecule releases two molecules of free fatty acid (and one molecule of monoglyceride):

$$\frac{dN_{FFA}}{dt} = -2\frac{dN_{TG}}{dt} \quad (2)$$

where $\frac{dN_{TG}}{dt}$ is the number of moles of TG lost from the oil droplet per unit time due to lipolysis and solubilization, with N_{TG} the number of TG moles in the oil droplet (mol).

From eqs (1), (2) we have

$$k_S S = -2\frac{dN_{TG}}{dt} \quad (3)$$

The number of TG moles can be related to the droplet volume as:

$$N_{TG} = \frac{V\rho}{M_W} \quad (4)$$

where V is the volume of the triglyceride oil droplet (m^3), ρ is the density of the triglyceride oil droplet (g m^{-3}), assumed to be constant throughout digestion, and M_W is the molecular weight of the triglyceride oil (g mol^{-1}).

From eqs. (3) and (4), we have:

$$k_S S = -2\frac{\rho}{M_W}\frac{dV}{dt} \quad (5)$$

as $S = 4\pi R^2$ and $V = 4/3\,\pi R^3$, R being the radius of the oil droplet (m). Substituting S and V in eq. (5) leads to:

$$k_S 4\pi R^2 = -2\frac{\rho}{M_W}\frac{dV}{dR}\frac{dR}{dt} = -2\frac{\rho}{M_W}4\pi R^2\frac{dR}{dt} \qquad (6)$$

Simplifying eq. (6) leads to:

$$k_S = -2\frac{\rho}{M_W}\frac{dR}{dt} \qquad (7)$$

for which a solution can be calculated to be:

$$R(t) = R_0\left(1 - \frac{k_S M_W}{2R_0\rho}t\right) \qquad (8)$$

For N_{FFA} (t), a solution was calculated in the literature (Li & Mcclements, 2010; Marze & Choimet, 2012; Gaucel et al., 2015):

$$N_{FFA}(t) = 2N_{TG,total}\left[1 - \left(1 - \frac{k_S M_W}{2R_0\rho}t\right)^3\right] \qquad (9)$$

Assuming the FFA release rate is proportional to the surface area of the oil droplet per unit total reaction volume (specific surface area), eqs. (8) and (9) can be rewritten as:

$$R(t) = R_0\left(1 - \frac{k_{SV} M_W}{2R_0\rho V_T}t\right) \qquad (10)$$

$$N_{FFA}(t) = 2N_{TG,total}\left[1 - \left(1 - \frac{k_{SV} M_W}{2R_0\rho V_T}t\right)^3\right] \qquad (11)$$

where V_T is the total reaction volume (m^3), that is the volume of both the oil and the aqueous phases, and k_{sv} is the FFA release rate per unit specific droplet surface area (mol m s^{-1}).

References

Li, Y., & Mcclements, D. J. (2010). New mathematical model for interpreting ph-stat digestion profiles: Impact of lipid droplet characteristics on in vitro digestibility. *Journal of Agricultural and Food Chemistry*, *58*(13), 8085–8092.

Marze, S., & Choimet, M. (2012). In vitro digestion of emulsions: Mechanistic and experimental models. *Soft Matter*, *8*(42), 10982–10993.

Gaucel, S., Trelea, I. C., & Le Feunteun, S. (2015). Comment on New Mathematical Model for Interpreting pH-Stat Digestion Profiles: Impact of Lipid Droplet Characteristics on in Vitro Digestibility, *3*(4), 4–5.

pH-stat measurements for emulsions

The digestion degree of emulsions was measured by the pH-stat method with buffer and ionization corrections (Chatzidaki et al., 2016).

Emulsions (2 wt% oil) of different oils (TC or HOSO or fish oil) were prepared. The aqueous phase (2 mg mL^{-1} beta-lactoglobulin) was prepared by mixing the protein in 10 mM NaH_2PO_4 buffer solution (pH 7.0) for 30 min at room temperature. A rotor-stator homogenizer (Silent Crusher M, Heidolph Instruments, Germany) was used for a pre-emulsification step (2 min, 16000 rpm). Then, a fine emulsion was obtained by sonication (Misonix Sonicator 4000, Qsonica, USA) applied for 3 cycles of 1 min (total energy 2100 J). A 2 min cooling time was applied between each cycle. The droplet size distributions of the emulsions were measured using dynamic light scattering (Zetasizer Nano ZS, Malvern Instruments, UK) equipped with a He-Ne laser of wavelength 633 nm. The volume-based mean droplet diameters were found to be of 265±38, 313±43, and 351±48 nm for TC, HOSO, and fish oil emulsions, respectively.

Emulsions were diluted 2 fold with a gastric buffer solution (130 mM NaCl, 1.6 mM $CaCl_2.(H_2O)_2$, pH 3.0) to mimic the gastric dilution. The digestion was started by diluting the gastric emulsion 2 fold in the intestinal fluid (130 mM NaCl, 1.6 mM $CaCl_2.(H_2O)_2$, pH 7.0) containing 0.2 mg mL^{-1} pancreatic lipase (L3126) and 20 mg mL^{-1} bile extract (B8631, about 50 wt% bile salts). FFA release was measured in duplicate with a pH-stat titrator at 37 °C (TitraLab 90, Radiometer, Denmark). The results are shown in the figure below.

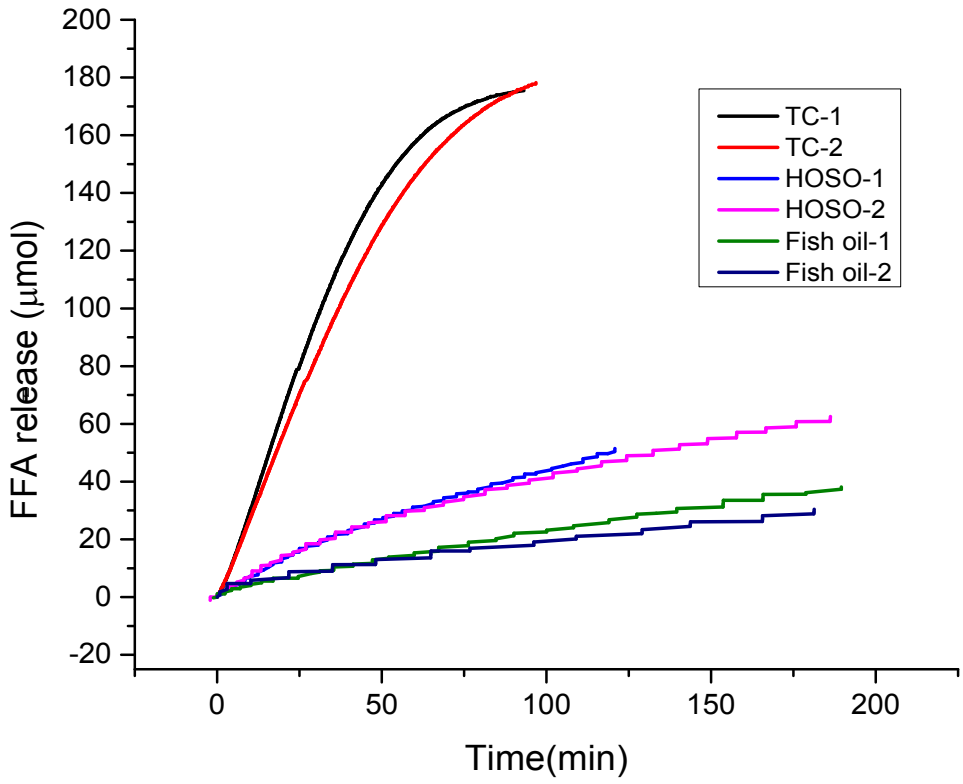

FFA release during intestinal digestion for different oils in emulsion, measured by the pH-stat method.

By fitting these data with eq. (9) of supplementary material S3, we obtained the FFA release rate per unit surface area, which we compared to the values obtained for the microfluidic experiments (table 1). The values for the pH-stat are in good agreement with our previous results (Marze, & Choimet, 2012), but much lower than those reported by Li and McClements (2010). This is likely related to the much lower concentrations of lipase and calcium we used compared to these authors. It is indeed known that the lipolysis rate is increased by both lipase and calcuim concentrations. The pH-stat values are also much lower than the microfluidic values. As already discussed, this can be due to a coalescence process for emulsions, but it is unlikely to explain alone such a large difference.

Table 1: FFA release rate per unit surface area of the oil droplets.

Oil	FFA release rate by the pH-stat method (μmol s^{-1} m^{-2})	FFA release rate by the microfluidic method (μmol s^{-1} m^{-2})
TC	$68\times10^{-3} \pm 7\times10^{-3}$	41.2 ± 1.4
HOSO	$10.5\times10^{-3} \pm 0.8\times10^{-3}$	13.2 ± 0.2
Fish oil	$5.1\times10^{-3} \pm 0.8\times10^{-3}$	3.08 ± 0.01

The pH-stat data were also fitted with eq. (11) of supplementary material S3 to evaluate the effect of the total reaction volume. The FFA release rate per unit specific surface area are compared in table 2 with the values fitted for the microfluidic experiments using eq. (10). The values are now much closer (related by a factor 2.4, or in the same range for HOSO). It is thus clear that the total reaction volume is an essential parameter to compare experiments at different scales.

Table 2: FFA release rate per unit specific surface area of the oil droplets.

Oil	FFA release rate by the pH-stat method (μmol μL s^{-1} m^{-2})	FFA release rate by the microfluidic method (μmol μL s^{-1} m^{-2})
TC	544 ± 56	226.6 ± 7.7
HOSO	84.0 ± 6.4	72.6 ± 1.1
Fish oil	40.8 ± 6.4	16.94 ± 0.06

Finally, we analyzed the pH-stat data by the standard enzyme activity calculation, using the initial maximal slope (μmol min^{-1}) of the FFA release curve, normalized by the mass of lipase in the reaction volume (μmol FFA min^{-1} mg^{-1} lipase, usually abbreviated to U mg^{-1}). The value of 0.84 U mg^{-1} for HOSO is about 2 fold lower than the minimal value reported by the manufacturer for olive oil. This result is nevertheless reasonable as the protocol of the manufacturer (Sigma) is unknown except for the pH which is 7.7, but overall should be similar.

Knowing the total number of moles of TG in the reaction volume, we also calculated a maximal molar percentage (% min^{-1}) of FFA release from the initial maximal slope. To compare with the microfluidic data, we derived an equation based on the same assumption:

$$\frac{dN_{FFA}}{dt} = kN_{FFA,total} = -2\frac{dN_{TG}}{dt} = -2kN_{TG,total} \quad (1)$$

As $N_{TG,total} = \frac{V_0\rho}{M_W}$, then we have:

$$\frac{dV}{dt} = kV_0 \quad (2)$$

which we can integrate to find:

$$V(t) = V_0(1 - kt) \quad (3)$$

where *k* is the FFA release rate (in min^{-1}). Eq. (3) was used to fit the maximal slope in the decrease of the normalized droplet volume, multiplied by 100 to obtain the value in % min^{-1}. The maximal BC release rate was also calculated by using the maximal slope of the normalized release curve, converted to % min^{-1}. The results are given in table 3, showing that this simple model, although not representing correctly the release curves that are not strictly linear, reconciles the data for both experiments. This means that the release rate in mol min^{-1} can be seen as driven by the total amount of TG, faster for a higher amount. The maximal BC release is also found to have similar values in % min^{-1}, not significantly different from those for FFA in the microfluidic experiments, and in the same range than that reported by Mutsokoti et al. (2017). Although the whole real-time kinetics of FFA and BC release were found to be distinct, using the maximal rate values confirms that some specific regimes obey the same kinetics.

Table 3: Maximal lipase activity and FFA release rate for the pH-stat experiments, FFA and BC release rates for the microfluidic experiments.

Oil	Maximal lipase activity by the pH-stat method (µmol FFA min^{-1} mg^{-1} lipase)	Maximal FFA release rate by the pH-stat method (% min^{-1})	Maximal FFA release rate by the microfluidic method (% min^{-1})	Maximal BC release rate by the microfluidic method (% min^{-1})
TC	3.7 ± 0.3	1.8 ± 0.2	2.8 ± 0.2	3.0 ± 0.4
HOSO	0.84 ± 0.01	0.71 ± 0.01	1.3 ± 0.2	1.42 ± 0.02
Fish oil	0.27 ± 0.03	0.38 ± 0.03	0.45 ± 0.07	0.55 ± 0.15

References

Li, Y., & Mcclements, D. J. (2010). New mathematical model for interpreting ph-stat digestion profiles: Impact of lipid droplet characteristics on in vitro digestibility. *Journal of Agricultural and Food Chemistry*, *58*(13), 8085–8092.

Marze, S., & Choimet, M. (2012). In vitro digestion of emulsions: Mechanistic and experimental models. *Soft Matter*, *8*(42), 10982–10993.

Chatzidaki, M. D., Mateos-Diaz, E., Leal-Calderon, F., Xenakis, A., & Carrière, F. (2016). Water-in-oil microemulsions versus emulsions as carriers of hydroxytyrosol: an in vitro gastrointestinal lipolysis study using the pHstat technique. *Food Funct.*, *7*(5), 2258–2269.

Mutsokoti, L., Panozzo, A., Pallares Pallares, A., Jaiswal, S., Van Loey, A., Grauwet, T., & Hendrickx, M. (2017). Carotenoid bioaccessibility and the relation to lipid digestion: A kinetic study. Food Chemistry, 232, 124–134.